IEICE Proceeding Series

# Evaluation of Topological Statistics of Retinotopic Brain Functional Networks

Kenji Leibnitz, Tetsuya Shimokawa, Ferdinand Peper

Vol. 1 pp. 743-746
Publication Date: 2014/03/17
Online ISSN: 2188-5079

2012 International Symposium on Nonlinear Theory and its Applications
NOLTA2012, Palma, Majorca, Spain, October 22-26, 2012

# Evaluation of Topological Statistics of Retinotopic Brain Functional Networks

Kenji Leibnitz†, Tetsuya Shimokawa†, and Ferdinand Peper†

† Center for Information and Neural Networks (CiNet)
National Institute of Information and Communications Technology
1-3 Yamadaoka, Suita, Osaka, 565-0871 Japan
Email: {leibnitz, shimokawa, peper}@nict.go.jp

**Abstract**—Functional networks describe the dependence of spatially distributed areas of the brain based on temporal correlations. In this paper, we discuss how functional networks generated from the time series of voxels in an fMRI experiment vary over time in response to a periodic retinotopic stimulation. Since functional connectivity studies only consider the entire experimental time series, there is usually only a single network constructed for each experiment and subject. Our goal is to investigate how the statistical properties of functional networks vary during an experiment and the relationship between the complex network measures.

## 1. Introduction

Brain functional networks express how different neural regions are jointly activated during an experimental measurement [1]. The *blood oxygen level dependent* (BOLD) hemodynamic response from neural activity is captured by functional MRI in the form of time series of voxels, which are three dimensional measurement units of 2–3 mm per side. The similarity in dynamics between two voxels $i$ and $j$ is in general compared through the correlation coefficient of their corresponding time series $v_i(t)$ and $v_j(t)$ [2], although other measures such as mutual information [3, 4], coherence [5], or other wavelet-based methods [6] have also been applied. In our case, we use the conservative definition over Pearson's correlation coefficient and if the correlation between two time series $v_i(t)$ and $v_j(t)$ lies above a threshold $r_c$, a strong relation among both voxels is assumed and a link is set in the adjacency matrix $A$, i.e., $A_{i,j} = 1$, otherwise $A_{i,j} = 0$. Since correlation is a symmetric operation, the resulting network is always undirected, i.e., $A_{i,j} = A_{j,i}$.

Most work in this area has focussed on networks for describing a stationary state of the brain, but in reality the brain is a plastic system that changes its dynamic relations depending on the input it receives. In this paper, our goal is to characterize how the typical complex network measures, e.g., node degree, characteristic path length, or modularity, change by segmenting the time axis into disjoint intervals corresponding to the same stimulation groups. Thus, we obtain various realizations of the same functional network for which we study the statistical properties of their measures, as well as the correlations among them to find relations that can not be identified from a single experimental trace.

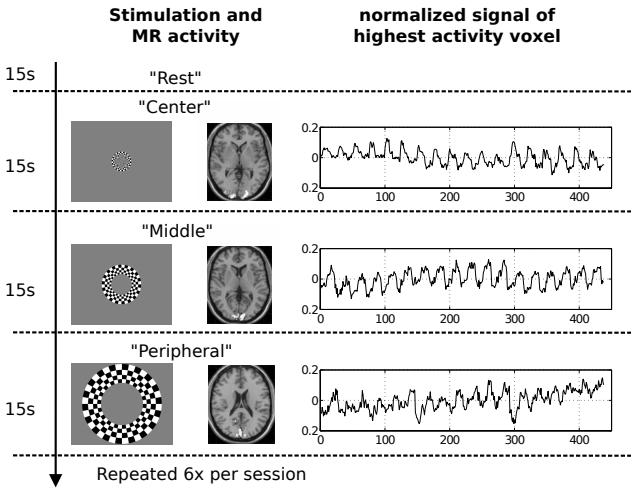


Figure 1: Overview of fMRI retinotopy experiment

The remainder of this paper is as follows. In Section 2, we briefly outline the experimental design and explain how the networks were extracted. Then, in Section 3 we summarize our evaluation, where we compare moments and correlations of the complex network measures, and show the statistics of a network aggregated over all extracted networks. Finally, this paper is concluded with Section 4.

## 2. Description of fMRI Experiment

We use in this study the same experimental data set that was introduced in our previous work [7]. The experiment consists of periodic stimulations of the primary visual cortex (V1) through flickering checkerboard annuli of three different sizes, denoted as "Center" (C), "Middle" (M), and "Peripheral" (P), followed by a "Rest" (R) epoch without stimulation. Each epoch has a duration of 6 scans of 2.5 s each and we denote one complete sequence of CMPR as a *group* of 24 scans. This is repeated 6 times within a *session* and the entire experiment comprises 3 sessions for 2 subjects. The F-values of the activation areas as output of the SPM software [8] for Matlab are depicted in Fig. 2, which shows as expected a high activation in the occipital region

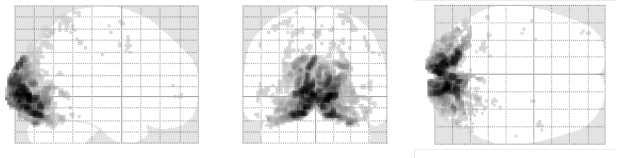

Figure 2: Output of F-test values of activation areas in V1 computed by SPM toolbox

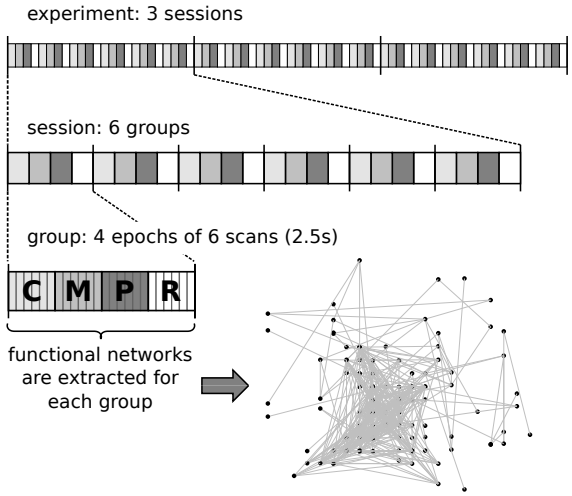


Figure 3: Layout of experiment with an extracted network from a CMPR group (coronal view). The primary visual area (V1) is densely interconnected by functional links.

where V1 is located.

Due to this regular experimental design, we split the entire time series into portions of recurring CMPR groups consisting of 24 scans each and construct a functional network by thresholding the correlation matrix of the time series of each voxel for each group instead of the whole time series, see Fig. 3. In order to reduce the size of the matrix, we limit ourselves to voxels taken at a sampling step size of 3 voxels in either dimension. The resulting 18 networks form the basis of our evaluation and for the sake of a better comparison, we varied the correlation coefficient threshold $r_c$ for each network such that there is a fixed number of $\ell = 500$ links. In other words, since the networks represent the same sequence of CMPR at different times, we can consider the network as stochastic quantity and the 18 obtained networks as realizations of this random variable.

From Fig. 4, we can recognize that while many networks have a common high connectivity in the occipital area, several networks also have a large number of links in other regions that are not involved in visual processing. This is quite likely caused by the short length of the 24 samples used for calculating the correlation coefficients.

Table 1: Average values of complex network measures. Numbers in parentheses indicate the coefficient of variation. Randomized networks were averaged over 100 repetitions.

| | **original** | | **randomized** | |
|---|---|---|---|---|
| nodes $n$ | 212.72 | (0.20) | 212.72 | (0.20) |
| modularity $Q$ | 0.64 | (0.16) | 0.44 | (0.18) |
| path length $L$ | 5.89 | (0.27) | 3.43 | (0.12) |
| assortativity $r$ | 0.25 | (0.45) | -0.08 | (-0.59) |
| clust. coef. $C$ | 0.28 | (0.20) | 0.07 | (0.82) |
| degree $\langle k \rangle$ | 4.74 | (0.24) | 4.74 | (0.24) |

## 3. Evaluation of Network Measures

We now perform a statistical evaluation of the extracted networks by studying their complex network measures. For the numerical evaluation, we used the Brain Connectivity Toolbox [9] in Matlab.

### 3.1. Moments of Network Measures

In the next step, we investigate standard complex network measures and try to quantify any fluctuations and correlations that these values show. For this, we use all 36 extracted networks of both subjects and construct each of them to have 500 links by varying the correlation threshold $r_c$. Furthermore, we compare the values to those of completely randomized networks having the same degree distribution as the original network. The results are summarized in Table 1.

From Table 1 we can recognize that the original brain networks have higher average values of modularity, assortativity, clustering coefficient, and path length. In fact, the randomized networks have almost no degree correlations (assortativity) and exhibit almost no noticeable clustering. The CDFs of modularity, assortativity, and clustering coefficient are exemplarily shown in Fig. 5.

### 3.2. Correlations between Metrics

Since we now have a series of values for each considered measure, we can identify any correlations between the values. This is shown in Tables 2a and 2b for the original and randomized networks, respectively.

We can recognize from these tables that there is a clear separation of local (clustering coefficient, degree) and global measures (nodes, modularity, characteristic path length) depending on their respective correlations. We can recognize two main differences in these tables. First, the correlations of assortativity and other measures differ significantly and even change their sign when comparing the original and randomized networks. Furthermore, the other measures have larger absolute values for both positive and negative correlations in randomized networks.

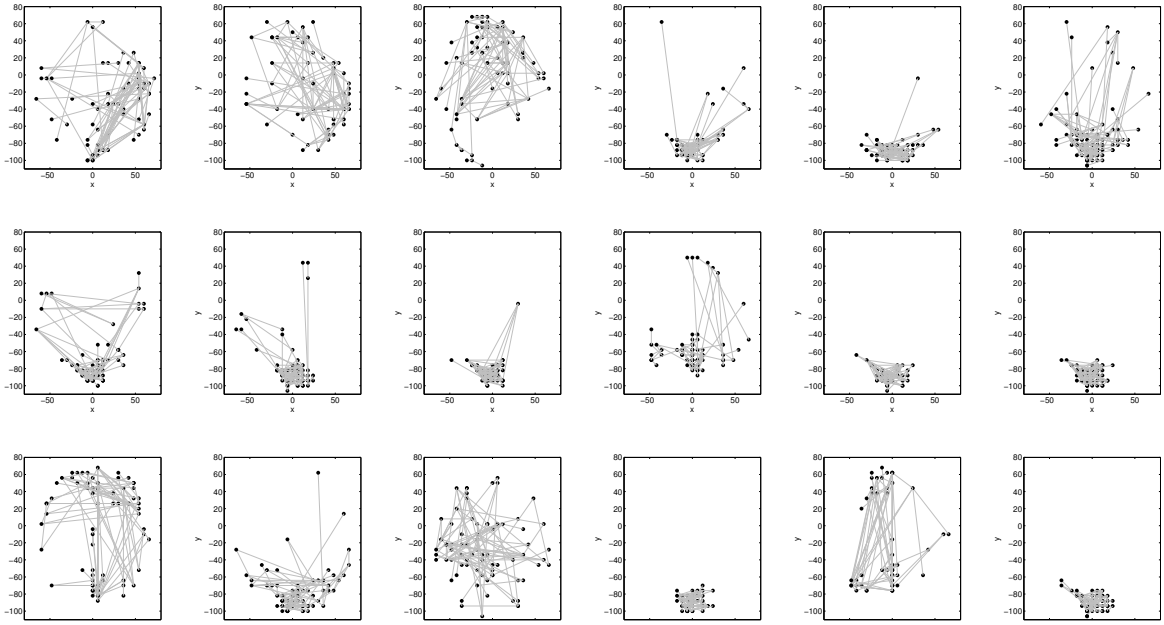

Figure 4: The 18 networks constructed from each CMPR group for Subject 1 (axial view). For sake of clarity, the threshold for each network was individually adjusted so that each resulting network has 100 links.

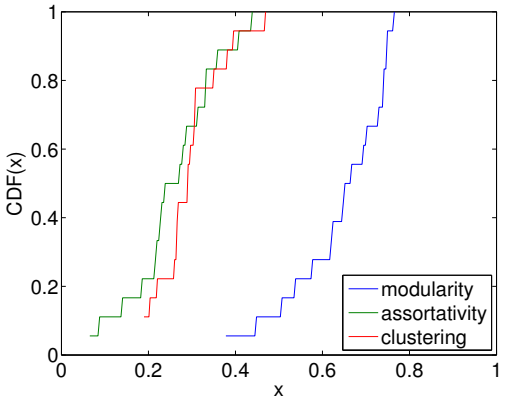


Figure 5: CDFs of modularity, assortativity, and clustering coefficient obtained from CMPR groups

### 3.3. Superposition of Networks

Although our goal was to generate separate realizations of networks in order to obtain their statistics, we can also compare the resulting structure after superimposing all generated CMPR networks. The sum of each of these 18 adjacency matrices $A^{(k)}$ of Subject 1, leads to a weighted matrix $A^* = \sum_k A^{(k)}$, where the weight represents the number of times the same link reappears among all networks. We then remove all links which are below a weight threshold $w'$ and obtain a common adjacency matrix $A' = \text{sign}(A^* > w')$. This is illustrated in Fig. 6 for Subject 1. It can be seen that for $w'$ of 3 or more, the resulting network matches well with the V1 area with activations in the occipital area of the brain, as can be seen from Fig. 2. This result shows that it is sufficient to only consider the time series segments of shorter lengths than the whole time series, if a large number of such groups is taken into account.

Table 2: Correlation coefficient of network measures ($\ell$ = 500 links). Differences in sign are highlighted in boldface.

(a) Original networks

| | $n$ | $Q$ | $L$ | $r$ | $C$ | $\langle k \rangle$ |
|---|---|---|---|---|---|---|
| $n$ | 1.00 | 0.79 | 0.54 | **-0.17** | -0.62 | -0.76 |
| $Q$ | 0.79 | 1.00 | 0.70 | **-0.03** | -0.60 | -0.88 |
| $L$ | 0.54 | 0.70 | 1.00 | 0.36 | -0.28 | -0.49 |
| $r$ | **-0.17** | **-0.03** | 0.36 | 1.00 | **0.19** | **0.10** |
| $C$ | -0.62 | -0.60 | -0.28 | **0.19** | 1.00 | 0.86 |
| $\langle k \rangle$ | -0.76 | -0.88 | -0.49 | **0.10** | 0.86 | 1.00 |

(b) Randomized networks

| | $n$ | $Q$ | $L$ | $r$ | $C$ | $\langle k \rangle$ |
|---|---|---|---|---|---|---|
| $n$ | 1.00 | 0.77 | 0.83 | **0.81** | -0.82 | -0.76 |
| $Q$ | 0.79 | 1.00 | 0.99 | **0.89** | -0.92 | -0.97 |
| $L$ | 0.83 | 0.99 | 1.00 | 0.89 | -0.90 | -0.95 |
| $r$ | **0.81** | **0.89** | 0.89 | 1.00 | **-0.98** | **-0.93** |
| $C$ | -0.83 | -0.92 | -0.90 | **-0.98** | 1.00 | 0.97 |
| $\langle k \rangle$ | -0.76 | -0.97 | -0.95 | **-0.93** | 0.97 | 1.00 |

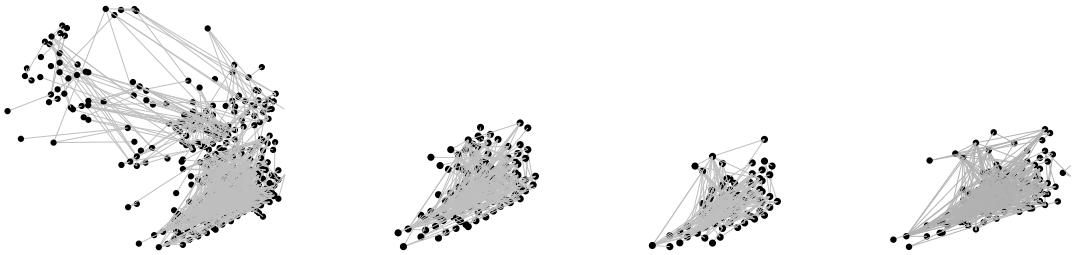

(a) $w' = 2$ (b) $w' = 3$ (c) $w' = 4$ (d) Entire time series

Figure 6: Thresholded sum of adjacency matrices. When removing all links with $w \leq 2$ from $A^*$, we get a good approximation of the entire V1 functional network for retinotopy. (a) $w' = 1$: 2821 nodes, 10296 links; (b) $w' = 2$: 344 nodes, 1552 links; (c) $w' = 3$: 129 nodes, 729 links; (d) entire time series.

## 4. Conclusion

In this paper we investigated brain functional networks generated from a repetitive experimental pattern. Instead of looking only at the entire time series, we segmented it into groups, which yielded multiple replications of the same functional network. Although the experimental design was the same in all cases, we obtained several variations of functional networks when projected to their anatomical coordinates in Fig. 4. This multiplicity permitted us, however, to evaluate statistical properties and correlations among the observed complex network measures. We recognized a distinct grouping of global and local network measures that are highly correlated with each other. Comparison with randomized networks showed much stronger correlation levels with changes of the sign of correlation than when comparing assortativity with the other metrics. Finally, we also showed that an aggregate view of the individual networks yielded a good approximation for the overall functional network.


## Acknowledgments

The authors would like to express their thanks to Yusuke Morito for his help in obtaining the fMRI data, as well as Tsutomu Murata and Hiroaki Umehara for the discussions.


## References


[1] O. Sporns, *Networks of the brain,* MIT Press, 2011.

[2] M.A. Kramer, U.T. Eden, S.S. Cash, E.D. Kolaczyk, "Network inference with confidence from multivariate time series", *Phys. Rev. E*, vol 79, 061916, 2009.

[3] W. Tedeschi, H.-P. Müller, D.B. de Araujo, A.C. Santos, U.P.C. Neves, S.N. Ernè, O. Baffa, "Generalized mutual information tests applied to fMRI analysis", *Physica A: Statistical Mechanics and its Applications*, vol. 352, no. 2–4, pp. 629–644, 2005.

[4] L. Deuker, E.T. Bullmore, M. Smith, S. Christensen, P.J. Nathan, B. Rockstroh, D.S. Bassett, "Reproducibility of graph metrics of human brain functional networks", *NeuroImage*, vol. 47, pp. 1460–1468, 2009.

[5] J.-P. Lachaux, A. Lutz, D. Rudrauf, D. Cosmelli, M. Le Van Quyen, J. Martinerie, F. Varela, "Estimating the time-course of coherence between single-trial brain signals: an introduction to wavelet coherence", *Neurophysiol. Clin.*, vol. 32, no. 3, pp. 157–74, 2002.

[6] E. Bullmore, J. Fadili, V. Maxim, L. Sendur, B. Whitcher, J. Suckling, M. Brammer, M. Breakspear, "Wavelets and functional magnetic resonance imaging of the human brain", *NeuroImage*, vol. 23, suppl. 1, 2004, pp. S234–S249, 2004.

[7] K. Leibnitz, T. Shimokawa, H. Umehara, T. Murata, "Topological comparison of brain functional networks and Internet service providers", *IEICE Trans. Comm.*, Special Section on Frontiers of Information Networks Science, vol. E95-B, no. 5, pp. 1539–1545, 2012.

[8] Wellcome Trust Centre for Neuroimaging, "Statistical Parametric Mapping (SPM)", available online at: `http://www.fil.ion.ucl.ac.uk/spm/`.

[9] M. Rubinov, O. Sporns, "Complex network measures of brain connectivity: Uses and interpretations," *NeuroImage*, vol. 52, pp. 1059-1069, 2010.